

Oliver Dudeck  
Martin Zeile  
Christian Wybranski  
Alice Schulmeister  
Frank Fischbach  
Maciej Pech  
Gero Wieners  
Ricarda Rühl  
Oliver Grosser  
Holger Amthauer  
Jens Ricke

## Early prediction of anticancer effects with diffusion-weighted MR imaging in patients with colorectal liver metastases following selective internal radiotherapy

Received: 19 February 2010  
Revised: 25 March 2010  
Accepted: 21 April 2010  
Published online: 20 June 2010  
© European Society of Radiology 2010

O. Dudeck (✉) · M. Zeile · C. Wybranski ·  
A. Schulmeister · F. Fischbach · M. Pech ·  
G. Wieners · R. Rühl · O. Grosser ·  
H. Amthauer · J. Ricke  
Department of Radiology and Nuclear  
Medicine,  
University of Magdeburg,  
Magdeburg, Germany  
e-mail: oliver.dudeck@med.ovgu.de  
Tel.: +49-391-6713030  
Fax: +49-391-6713029

**Abstract Objective:** To prospectively evaluate diffusion-weighted imaging (DWI) for early prediction of tumour response in patients with colorectal liver metastases following selective internal radiotherapy (SIRT).

**Methods:** We evaluated 41 metastases in 21 patients, age  $62.9 \pm 9.9$  years. All patients underwent magnetic resonance imaging (MRI) including breath-hold echoplanar DWI sequences. Imaging was performed before therapy (baseline MRI), 2 days after SIRT (early MRI) as well as 6 weeks later (follow-up MRI). Tumour volume (TV) and intratumoural apparent diffusion coefficient (ADC) were measured independently by two radiologists at all time points. **Results:** Metastases were categorised as responding lesions (RL;  $n=33$ ) or non-responding lesions (NRL;  $n=8$ ) according to changes in TV after

6 weeks. We found an inverse correlation of changes in TV and ADC at follow-up MRI with a Pearson's correlation coefficient of  $r=-0.66$  ( $p<0.0001$ ). On early MRI, no significant changes in TV were found for either RL or NRL. Conversely, ADC decreased significantly in RL by  $10.7 \pm 8.4\%$  ( $p<0.0001$ ). ADC increased in NRL by  $9.6 \pm 20.8\%$ , which was not statistically significant ( $p=0.40$ ). **Conclusion:** DWI was capable of predicting therapy effects of SIRT in patients with colorectal hepatic metastases as early as 2 days following treatment.

**Keywords** Colorectal liver metastases · Diffusion-weighted imaging · Prediction · Selective internal radiotherapy · Tumour response

### Introduction

Selective internal radiotherapy (SIRT) with intra-arterial administration of  $^{90}\text{Y}$  microspheres is a promising treatment in patients with colorectal liver metastases [1–3]. At the moment this method is most commonly applied in patients with unresectable and chemorefractory lesions as a salvage therapy. Currently, the value of SIRT at an earlier stage is under investigation in a multicentric randomised phase III trial and will most likely result in an increased need for follow-up with cross-sectional imaging [4]. However, traditional criteria used to assess

tumour response may not be conclusive until 3 months after therapy [3, 5]. Hence, there is a need for a non-invasive imaging method to determine therapeutic effectiveness at an earlier stage, which would allow clinicians to make early adjustments in treatment strategy and thus optimise individual patient therapy.

Diffusion-weighted magnetic resonance imaging (DWI) may represent such a surrogate imaging biomarker to presage changes in tumour response by means of quantification of tissue water mobility [6–8]. The apparent diffusion coefficient (ADC), which is the quantitative parameter of DWI, can be used to determine the presence

of highly cellular or acellular regions within a tumour, which can be used for the assessment of the effectiveness of anticancer treatment [7, 9, 10].

Abdominal DWI has, in the past, been hampered by technical challenges, mostly related to the heterogeneity of the magnetic field, low spatial resolution as well as image distortion as a result of motion sensitivity and susceptibility variation. These limitations have significantly complicated routine clinical DWI of the visceral organs. However, owing to improvement, the technique has increasingly been used in the liver for detection and characterisation of hepatic lesions [11–13] as well as prediction and monitoring of outcomes of anticancer therapies [14–21].

The purpose of this study was to test the hypothesis that DWI can presage tumour response in patients with colorectal liver metastases as early as 2 days after administration of  $^{90}\text{Y}$  microspheres.

## Materials and methods

### Patient population

The study was approved by the local institutional review board and written informed consent was obtained from each patient. Between June 2008 and July 2009, 21 patients (nine women and 12 men; mean age  $62.9 \pm 9.9$  years; range: 44–75 years) with a total of 41 unresectable colorectal liver metastases who successfully underwent SIRT were enrolled in this prospective trial. Inclusion criteria were well assessable metastatic lesions on initial MRI, for which ADC values could be determined on at least three consecutive sections. Lesions that were confluent or could not be sufficiently evaluated on follow-up MRI (e.g. as a result of tumour shrinkage with consecutive inappropriate delineation on DW images) or were not located within the Bremsstrahlung imaging performed after administration of  $^{90}\text{Y}$  microspheres had to be excluded. In order to minimise bias, no more than three lesions per patient were included, which were picked randomly. In most patients only lesions in the lobe in which SIRT was applied first were included (in 13 patients, right liver lobe treatment first, and in eight patients, left liver lobe treatment first) but in three patients, lesions of both lobes were included.

Surgical pre-treatment comprised hemihepatectomy in two and atypical lobectomy in another two patients. In one patient, who underwent hemihepatectomy, whole-liver radiation was also performed. All patients had received systemic chemotherapy before SIRT (mean number of chemotherapy regimens  $3.5 \pm 1.7$ ; range: 1–7). Fourteen patients (77.8%) had also been treated with monoclonal antibodies. None of the patients received concomitant or adjuvant chemotherapy within the follow-up period.

### MR technique

Magnetic resonance examinations were performed with a 1.5-T MR system (Gyrosan, Intera, Phillips Medical Systems, Best, The Netherlands) employing a SENSE torso surface coil. Imaging was performed at three time-points: immediately before SIRT (baseline MRI; performed  $5.9 \pm 6.2$  days before SIRT), 2 days (early MRI; mean  $2.1 \pm 0.7$  days) and 6 weeks after SIRT (follow-up MRI; mean  $45.4 \pm 11.5$  days). Unenhanced  $T_1$ -weighted (gradient echo, TR=211 ms, TE=3.3 ms, 450-cm FOV,  $256 \times 144$  matrix, SENSE factor 2, section thickness 8 mm) and  $T_2$ -weighted fast spin echo (TR=1,600 ms, TE=100 ms,  $\alpha=80^\circ$ , 450-cm FOV,  $384 \times 196$  matrix, SENSE factor 2, section thickness 8 mm) axial imaging were performed before DWI and Gd-EOB-DTPA contrast medium administration.

Breath-hold axial single shot echo planar (EPI) DWI was performed using the following parameters: TR=1,850 ms; TE=68 ms;  $b$  factors 0 and  $500 \text{ s/mm}^2$ ;  $112 \times 111$  matrix size, 450-cm FOV; section thickness 8 mm; NSA 2; half scan factor 0.608. Twelve sections through the liver were acquired in each 20-s breath-hold, and the entire liver (from the level of the diaphragm to the inferior edge of liver) was evaluated in two to three breath-holds. ADC maps were calculated on a voxel-by-voxel basis with an algorithm implemented according to the following equation:

$$\text{ADC} (\text{mm}^2\text{s}^{-1}) = [\ln(S^0/S^b)]/b$$

where  $S^0$  and  $S^b$  represent the signal intensities of the images with different gradient  $b$  factors, and  $b$  is the difference between gradient  $b$  factors.

Then, 0.1 mmol/kg body weight of Gd-EOB-DTPA (Primovist; Schering, Berlin, Germany) was administered with an infusion rate of 1.5 ml/s followed by a 30-ml saline flush.  $T_1$ -weighted three-dimensional (3D) turbo field echo (TFE) imaging sequences were acquired with the following parameters: TR=3.9 ms, TE=1.9 ms,  $\alpha=10^\circ$ , 450-cm FOV,  $192 \times 136$  matrix, SENSE factor 2, section thickness 6 mm, spectral adiabatic inversion recovery (SPAIR). In order to minimise differences in contrast media circulation time, the first post-contrast (arterial phase) sequence was started manually by using the bolus-tracking technique at the time when contrast agent reached the ascending aorta, typically 14–17 s after the start of injection. For subsequent acquisitions, intervals allowing patient's free breathing were placed between the arterial and portal venous phases (20 s) and the portal venous and equilibrium (i.e. interstitial) phases (40 s), respectively.  $T_1$ -weighted 3D TFE as well as  $T_1$ -weighted fast spin echo (FSE) images (TR=131 ms, TE=5 ms,  $\alpha=70^\circ$ , 450-cm FOV,  $256 \times 135$  matrix, SENSE factor 2, section thickness 8 mm) at the hepatocyte-selective (delayed) phase were acquired 10–20 min after contrast material administration.

## Technique of administration of $^{90}\text{Y}$ microspheres

For each patient, angiography with catheterisation of the coeliac trunk was performed to evaluate vascular and liver tumour anatomy as well as blood flow dynamics. Coil embolisation of vessels deriving from the hepatic artery not supplying the liver was performed. Typically, these vessels were the gastroduodenal artery, the right gastric artery as well as the cystic artery. Technetium $^{99\text{m}}$  macro-aggregated albumin (MAA) imaging was performed to test for residual gastrointestinal flow and to estimate the percentage of injected activity shunting to the lungs. The required activity to be injected and the dose received by the liver and lungs were calculated according to previously reported methods [22].

At a median of  $20 \pm 16$  days after this procedure,  $^{90}\text{Y}$  microspheres (Sirtex Medical, Lane Cove, Australia) were administered via a microcatheter placed in a lobar or segmental branch of the hepatic artery. SIRT was performed as a sequential treatment of each liver lobe in order to reduce the risk of radiation-induced liver disease. The time interval between right and left liver lobe treatment was  $35 \pm 5.7$  days. Right liver lobe treatment was performed with a median dose of  $1,200 \pm 150$  MBq (range: 800–1,200 MBq), left liver lobe treatment with a dose of  $800 \pm 220$  MBq (range: 350–1,000 MBq; activity of 50 Bq/sphere). In the case of previous hemihepatectomy  $^{90}\text{Y}$  microspheres were also administered sequentially in two sessions as a segmental SIRT of the remaining liver lobe. One SIRT of the left liver lobe was performed superselectively with a dose of 350 MBq. Afterwards, Bremsstrahlung imaging was performed to confirm the technical success of lobar SIRT.

## Imaging analysis

Study lesions were depicted in consensus by three experienced radiologists in MR imaging (G.W., F.F., and O.D.). Afterwards, two radiologists (M.Z. and O.D.) assessed tumour volume (TV), the mean apparent diffusion coefficient (ADC) of each lesion on baseline MRI, early MRI and follow-up MRI as well as tumour vascularisation on initial angiograms.

Tumour volume expressed in cubic centimetres ( $\text{cm}^3$ ) was assessed by segmentation of transversal contrast-enhanced T $_1$ -weighted images. The tumour border was defined manually and the area was automatically calculated by the workstation (Infinit, Seoul, Korea). Tumour volume was calculated according to the following equation:

$$V = s \cdot (a_1 + a_2 + a_3 + \dots + a_n)$$

( $s$ : section interval,  $a_1 - a_n$ : area of section)

These volumetric measurements were performed twice by two independent investigators and the mean of all

measurements was recorded as a representative value for each case.

ADC maps were calculated on a voxel-by-voxel basis with an algorithm implemented according to the following equation:

$$\text{ADC} (\text{mm}^2\text{s}^{-1}) = [\ln(S^0/S^b)]/b,$$

where  $S^0$  and  $S^b$  represent the signal intensities of the images with different gradient  $b$  factors, and  $b$  is the difference between gradient  $b$  factors. The section with the largest tumour diameter was selected for ADC calculation. On that image, as well as on two adjacent images, an ROI as large as possible, without risking partial volume effects, was selected. These measurements were performed twice by two independent investigators and the mean of all measurements was recorded as a representative value for each case. Initial and follow-up images were matched and ADC calculations were performed on corresponding sections on follow-up MRI.

In addition, the angiographic degree of tumour vascularisation was rated according to a semi-quantitative scale (0 = none, 1 = weak, 2 = moderate, 3 = strong) by consensus of two investigators.

## Statistical analysis

Statistical analysis was performed using SPSS 15. Data are given as mean  $\pm$  standard deviation for continuous data, or as percentages for discrete variables. To test for interobserver measurement differences, Kendall's test of concordance was used. Data were compared using either the Wilcoxon test for comparisons of parameters within the same group (responding lesions/non-responding lesions) or the Mann-Whitney test for intergroup comparisons. Pearson's correlation coefficient was obtained to express the relationship between changes in ADC values and tumour volumes. A  $p$  value of 0.05 was set to be the level of statistical significance.

## Results

A total of 41 colorectal hepatic metastases were evaluated in terms of TV and intralesional ADC. No statistical differences in lesion volume measurements among observers were noted with Kendall's coefficients of concordance of 0.97, 0.95 and 0.91 for lesions at baseline, early and follow-up MRI, respectively. Similarly, high degrees of agreement were found for ADC measurements with Kendall's coefficients of 0.91, 0.88 and 0.90 for lesions at baseline, early and follow-up MRI, respectively.

According to changes in tumour volume on follow-up MRI, metastases were categorised as either responding

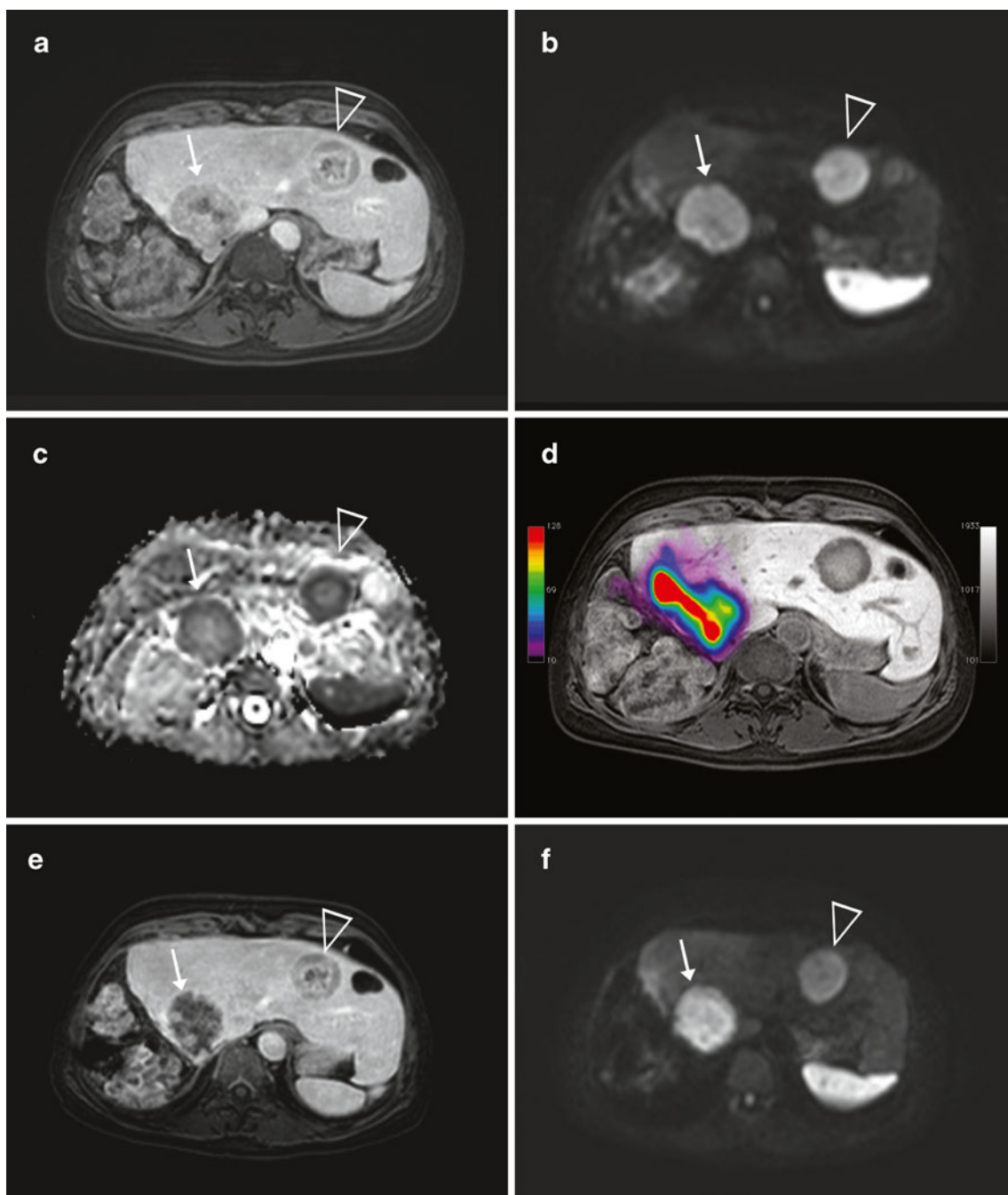


**Fig. 1a–j** A 66-year-old woman with new colorectal liver metastases following right hemihepatectomy scheduled for selective internal radiotherapy (SIRT). Pre-treatment T<sub>1</sub>-weighted Gd-EOB-DTPA-enhanced MR image (a), diffusion-weighted image (DWI) with  $b=500$  s/mm<sup>2</sup> (b) and corresponding ADC map (c) depict a metastasis at the resection border with a mean ADC of  $1.50 \times 10^{-3}$  mm<sup>2</sup>s<sup>-1</sup> (arrow) as well as a more peripherally located lesion with a mean ADC of  $138 \times 10^{-3}$  mm<sup>2</sup>s<sup>-1</sup> (arrowhead). It was decided that SIRT would be performed in two sessions in order to prevent radiation-induced liver disease. Bremsstrahlung imaging (d) shows the distribution of <sup>90</sup>Y microspheres after the first treatment. Note that only the lesion at the surgical resection border is treated with the first SIRT (arrow). Early

T<sub>1</sub>-weighted Gd-EOB-DTPA-enhanced MR image (e), DWI with  $b=500$  s/mm<sup>2</sup> (f), and ADC map (g) performed 2 days following SIRT reveal no relevant change in size of the treated lesion, but a decrease in the mean ADC by 14.0% to  $1.29 \times 10^{-3}$  mm<sup>2</sup>s<sup>-1</sup> (arrow). Also note the decrease in contrast enhancement of the tumour margin. The mean ADC of the untreated lesion is  $145 \times 10^{-3}$  mm<sup>2</sup>s<sup>-1</sup> (arrowhead). T<sub>1</sub>-weighted Gd-EOB-DTPA enhanced MR image (h), DWI with  $b=500$  s/mm<sup>2</sup> (i), and ADC map (j) performed 6 weeks later shows a decrease in the tumour volume by 33.5%. This finding correlates with a rise in the mean ADC of 52.7% to  $2.29 \times 10^{-3}$  mm<sup>2</sup>s<sup>-1</sup> (arrow). The mean ADC of the untreated lesion is  $133 \times 10^{-3}$  mm<sup>2</sup>s<sup>-1</sup>, which displays an increase in tumour size (arrowhead)

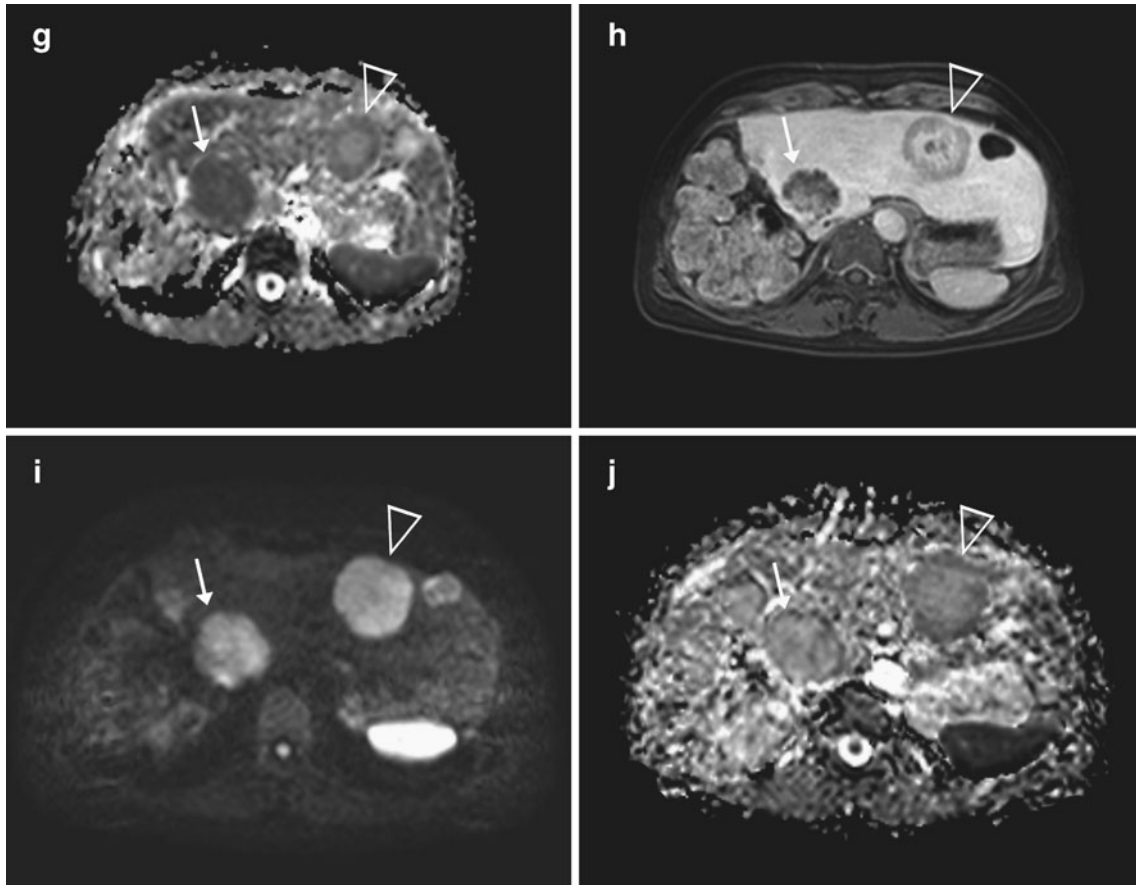


Fig. 1 (continued)

lesions (RL), if TV decreased, or non-responding lesions (NRL), if TV increased. Initial TV of RL ( $n=33$ ) was  $56.1 \pm 84.6 \text{ cm}^3$  (range:  $6.7\text{--}457.6 \text{ cm}^3$ ) while TV of NRL ( $n=8$ ) was  $27.0 \pm 26.0 \text{ cm}^3$  (range:  $5.8\text{--}84.6 \text{ cm}^3$ ;  $p=0.523$ ). Baseline ADC of RL was  $1.75 \pm 0.27 \times 10^{-3} \text{ mm}^2 \text{ s}^{-1}$  (range:  $1.36\text{--}2.51 \times 10^{-3} \text{ mm}^2 \text{ s}^{-1}$ ), which was significantly higher than  $1.42 \pm 0.30 \times 10^{-3} \text{ mm}^2 \text{ s}^{-1}$  (range:  $0.95\text{--}1.94 \times 10^{-3} \text{ mm}^2 \text{ s}^{-1}$ ) in NRL ( $p=0.005$ ).

Thirty-three metastases (80.5%) were rated as RL, in which TV decreased significantly by  $31.3 \pm 21.3\%$  (range:  $3.7\text{--}270.4 \text{ cm}^3$ ) on follow-up MRI 6 weeks after SIRT ( $p<0.0001$ ). For these lesions, ADC increased significantly by  $21.4 \pm 16.4\%$  (range:  $1.75\text{--}2.08 \times 10^{-3} \text{ mm}^2 \text{ s}^{-1}$ ;  $p<0.0001$ ; compare Fig. 1). Conversely, eight metastases (19.5%) were rated as NRL, in which TV increased by  $49.0 \pm 31.9\%$  (range:  $8.7\text{--}138.4 \text{ cm}^3$ ;  $p=0.012$ ), while ADC decreased by  $9.9 \pm 10.7\%$  (range:  $1.41\text{--}1.25 \times 10^{-3} \text{ mm}^2 \text{ s}^{-1}$ ;  $p=0.036$ ). Hence, differences in ADC were inversely correlated with morphological changes, regardless of treatment effects on TV. An analysis using Pearson's correlation coefficient indicated a statistically significant linear relationship of  $r=-0.66$  ( $p<0.0001$ ; Fig. 2).

In 11 out of 21 patients (47.6%) more than one lesion was evaluated in one individual. Among them, all lesions were RL in six cases (54.5%), while in only one patient all lesions were NRL (9.1%). Interestingly, we found RL as well as NRL in four individuals (36.4%).

On early MRI performed 2 days following SIRT, no significant changes in TV were found either for RL ( $14.0 \pm 8.0\%$ ; mean value:  $58.8 \pm 85.0 \text{ cm}^3$ ; range:  $6.8\text{--}444.7 \text{ cm}^3$ ;  $p=0.21$ ) or for NRL (mean value:  $28.4 \pm 27.8 \text{ cm}^3$ ;  $5.2 \pm 3.5\%$ ; range:  $6.3\text{--}91.6 \text{ cm}^3$ ;  $p=0.53$ ). Conversely, in RL a significant decrease in ADC of  $10.7 \pm 8.4\%$  (mean value:  $1.57 \pm 0.33 \times 10^{-3} \text{ mm}^2 \text{ s}^{-1}$ ; range:  $128.3\text{--}247.0 \times 10^{-3} \text{ mm}^2 \text{ s}^{-1}$ ) was found ( $p<0.0001$ ; Fig. 3). In 24 of 33 RL (72.7%) ADCs at early MRI were at least 5% lower compared with baseline values. ADC values of NRL displayed an increase of  $9.6 \pm 20.8\%$  (mean value:  $1.52 \pm 0.25 \times 10^{-3} \text{ mm}^2 \text{ s}^{-1}$ ; range:  $110.7\text{--}188.0 \times 10^{-3} \text{ mm}^2 \text{ s}^{-1}$ ), but no level of statistical significance was reached ( $p=0.40$ ; Fig. 4). Nevertheless, in six of eight NRL (75.0%) ADCs at early MRI were at least 5% higher compared with baseline values. Tumour response to administration of  $^{90}\text{Y}$  microspheres was independent of lesion vascular-

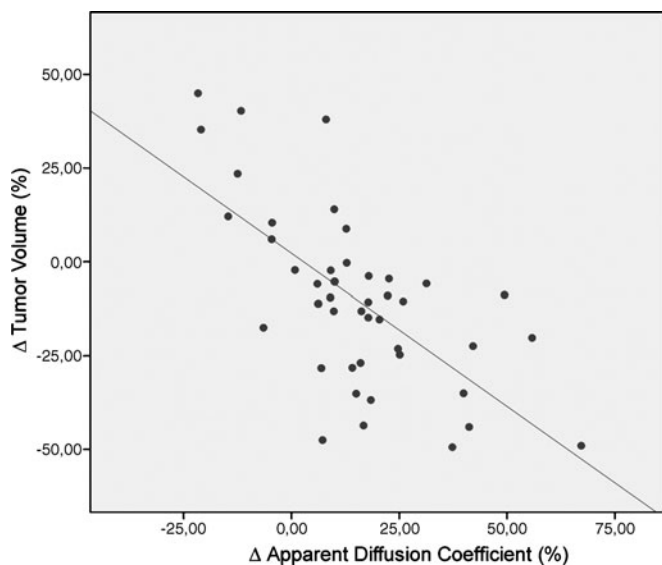


**Fig. 2** Relationship between changes in tumour volumes and ADC values. A decrease in tumour size is associated with an increase in ADC and vice versa. Pearson's correlation coefficient is  $r=-0.66$  and shows a significant linear relationship ( $p<0.0001$ )

isation at baseline as no differences were found for RL ( $2.03\pm 0.85$ ) and NRL ( $2.25\pm 0.89$ ;  $p=0.617$ ).

## Discussion

Our study demonstrated DWI to reveal significant increases in ADC values of RL 6 weeks after administration of  $^{90}\text{Y}$  microspheres. These results were in

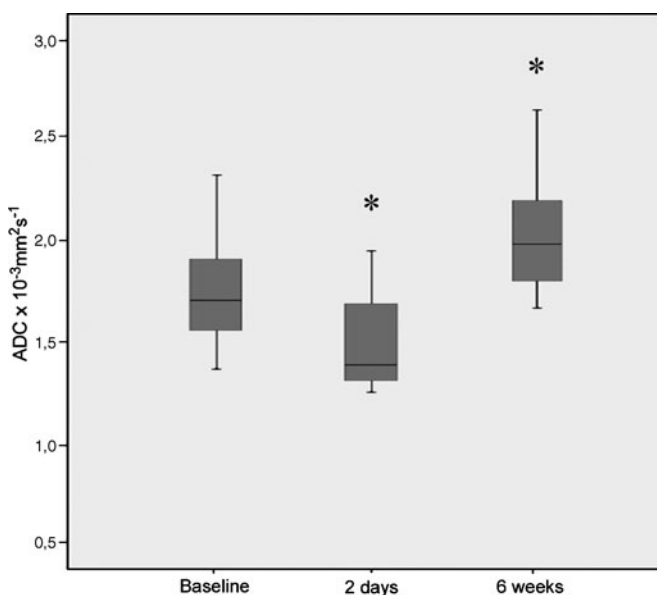


**Fig. 3** Box-and-whisker plot showing the percentage of changes for ADC values in responding lesions at baseline, 2 days and 6 weeks after administration of  $^{90}\text{Y}$  microspheres. ADC values decrease by  $10.7\pm 8.4\%$  at 2 days ( $p<0.0001$ ; asterisk) and increase by  $21.4\pm 16.4\%$  at 6 weeks ( $p<0.0001$ ; asterisk)

agreement with the current understanding of therapy-induced changes assessed by DWI: effective anticancer treatment results in tumour lysis, loss of cell membrane integrity, increased extracellular space, and, therefore, an increase in water diffusion [23, 24]. Our results were also well in accordance with results of previous studies of primary and secondary liver tumours, which have all shown an increase in ADC after a number of different therapeutic techniques [14, 15, 17–19, 21, 25]. Moreover, a significant decrease in ADC was found in NRL at follow-up MRI. In summary, we observed an inverse correlation of tumour response and changes in ADC values with a Pearson's correlation coefficient of  $r=-0.66$  (compare Fig. 2). Again, this finding was in agreement with previous results [12].

On early MRI performed a mean of 2 days after SIRT, no significant changes in TV were found for either RL or NRL. Conversely, DWI was able to differentiate tumour response at this early stage following SIRT as only in RL did ADC values decrease significantly (compare Figs. 3 and 4). How may this decrease in ADC be explained? Current models of tumour response postulate cell swelling to occur soon after initiation of anticancer therapy, which can lead to a transient decrease in tumour ADC [10, 25, 26]. Later, this is followed by cell necrosis and lysis, resulting in an increase in ADC. Animal studies assessing very early cellular changes have also noted a decrease in intratumoural ADC in the first 36 h after commencement of anticancer therapy [27, 28].

However, this scheme does not consider the contribution of intravascular perfusion to the diffusion measure-

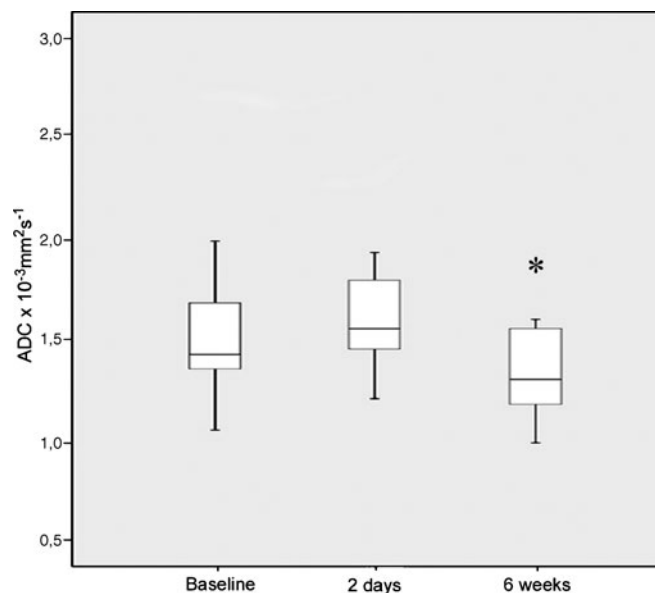


**Fig. 4** Box-and-whisker plot comparing the percentage of changes for ADC values in non-responding lesions at baseline, 2 days and 6 weeks after administration of  $^{90}\text{Y}$  microspheres. At 2 days ADC values increase by  $9.6\pm 20.8\%$ , which is not statistically significant ( $p=0.40$ ). At 6 weeks ADC values decrease by  $9.9\pm 10.7\%$  ( $p=0.036$ ; asterisk)

ment, which may be substantial in tumours as DWI provides simultaneous information on diffusion as well as microperfusion [29, 30]. Hence, therapies that are targeted against tumour vasculature such as SIRT may result in a reduction in ADC values, especially when DWI were acquired using low  $b$  values, which are influenced by tissue perfusion effects [26]. As colorectal metastatic liver lesions have variable vascularity, we also evaluated the angiographic tumour vascularity at baseline of all study lesions, but no significant difference was found for RL and NRL. Certainly, the use of an additional lower  $b$  value of 100–150 s/mm<sup>2</sup> to obtain information on tissue perfusion effects would have been beneficial [31], but scan times would have been unacceptably long for image acquisition during breath-hold. Besides, maybe a more precise assessment—for instance by MR perfusion—could provide further insights into the influence of SIRT on tumour perfusion.

Obviously, a key issue is timing of the evaluation of tumour response after the start of treatment. For the present study, we chose to perform MRI including DWI very early at a median of 2 days following SIRT. This

allowed us to obtain the first information on the treatment response before the patient was discharged, which is routinely 2 days after SIRT at our institution. As we observed RL and NRL within one individual in as many as 36.4% patients, such data may have clinical implications, e.g. thermal ablation of a single NRL in a patient with otherwise RL. Nevertheless, larger clinical studies have to confirm the ability of DWI to identify treatment response to anticancer therapy and identify the best time-point to perform early MRI before conclusions that influence the therapeutic strategy can be drawn. For this, we would suggest a more delayed time period, such as 2 weeks after SIRT, as immediate alteration of tumour perfusion due to the embolisation with <sup>90</sup>Y microspheres has the potential to affect quantitative ADC measurements.

In summary, DWI has great potential as an imaging biomarker for early prediction of tumour response in patients with colorectal liver metastases treated with SIRT. As patients also presented with mixed response, early recognition of tumour response is of particular clinical relevance in individuals with predominantly RL.

## References

- Welsh JS, Kennedy AS, Thomadsen B (2006) Selective Internal Radiation Therapy (SIRT) for liver metastases secondary to colorectal adenocarcinoma. *Int J Radiat Oncol Biol Phys* 66:S62–S73
- Lewandowski RJ, Thurston KG, Goin JE, Wong CY, Gates VL, Van Buskirk M, Geschwind JF, Salem R (2005) <sup>90</sup>Y microsphere (TheraSphere) treatment for unresectable colorectal cancer metastases of the liver: response to treatment at targeted doses of 135–150Gy as measured by [18F]fluorodeoxyglucose positron emission tomography and computed tomographic imaging. *J Vasc Interv Radiol* 16:1641–1651
- Salem R, Lewandowski RJ, Atassi B, Gordon SC, Gates VL, Barakat O, Sergie Z, Wong CY, Thurston KG (2005) Treatment of unresectable hepatocellular carcinoma with use of <sup>90</sup>Y microspheres (TheraSphere): safety, tumor response, and survival. *J Vasc Interv Radiol* 16:1627–1639
- Van Hazel G, Blackwell A, Anderson J, Price D, Moroz P, Bower G, Cardaci G, Gray B (2004) Randomised phase 2 trial of SIR-Spheres plus fluorouracil/leucovorin chemotherapy versus fluorouracil/leucovorin chemotherapy alone in advanced colorectal cancer. *J Surg Oncol* 88:78–85
- Koh DM, Padhani AR (2006) Diffusion-weighted MRI: a new functional clinical technique for tumour imaging. *Br J Radiol* 79:633–635
- Koh DM, Collins DJ (2007) Diffusion-weighted MRI in the body: applications and challenges in oncology. *AJR Am J Roentgenol* 188:1622–1635
- Chenevert TL, Meyer CR, Moffat BA, Rehemtulla A, Mukherji SK, Gebarski SS, Quint DJ, Robertson PL, Lawrence TS, Junck L, Taylor JM, Johnson TD, Dong Q, Muraszko KM, Brunberg JA, Ross BD (2002) Diffusion MRI: a new strategy for assessment of cancer therapeutic efficacy. *Mol Imaging* 1:336–343
- Taouli B, Koh DM (2010) Diffusion-weighted MR imaging of the liver. *Radiology* 254:47–66
- Ross BD, Moffat BA, Lawrence TS, Mukherji SK, Gebarski SS, Quint DJ, Johnson TD, Junck L, Robertson PL, Muraszko KM, Dong Q, Meyer CR, Bland PH, McConville P, Geng H, Rehemtulla A, Chenevert TL (2003) Evaluation of cancer therapy using diffusion magnetic resonance imaging. *Mol Cancer Ther* 2:581–587
- Dudeck O, Zeile M, Pink D, Pech M, Tunn PU, Reichardt P, Ludwig WD, Hamm B (2008) Diffusion-weighted magnetic resonance imaging allows monitoring of anticancer treatment effects in patients with soft-tissue sarcomas. *J Magn Reson Imaging* 27:1109–1113
- Bruegel M, Holzapfel K, Gaa J, Woertler K, Waldt S, Kiefer B, Stemmer A, Ganter C, Rummeny EJ (2008) Characterization of focal liver lesions by ADC measurements using a respiratory triggered diffusion-weighted single-shot echo-planar MR imaging technique. *Eur Radiol* 18:477–485
- Gourtsoyianni S, Papanikolaou N, Yarmenitis S, Maris T, Karantanis A, Gourtsoyiannis N (2008) Respiratory gated diffusion-weighted imaging of the liver: value of apparent diffusion coefficient measurements in the differentiation between most commonly encountered benign and malignant focal liver lesions. *Eur Radiol* 18:486–492
- Parikh T, Drew SJ, Lee VS, Wong S, Hecht EM, Babb JS, Taouli B (2008) Focal liver lesion detection and characterization with diffusion-weighted MR imaging: comparison with standard breath-hold T2-weighted imaging. *Radiology* 246:812–822
- Deng J, Miller FH, Rhee TK, Sato KT, Mulcahy MF, Kulik LM, Salem R, Omary RA, Larson AC (2006) Diffusion-weighted MR imaging for determination of hepatocellular carcinoma response to yttrium-90 radioembolization. *J Vasc Interv Radiol* 17:1195–1200
- Kamel IR, Bluemke DA, Ramsey D, Abusedera M, Torbenson M, Eng J, Szarf G, Geschwind JF (2003) Role of diffusion-weighted imaging in estimating tumor necrosis after chemoembolization of hepatocellular carcinoma. *AJR Am J Roentgenol* 181:708–710
- Koh DM, Scurr E, Collins DJ, Pirgon A, Kanber B, Karanjia N, Brown G, Leach MO, Husband JE (2006) Colorectal hepatic metastases: quantitative measurements using single-shot echo-planar diffusion-weighted MR imaging. *Eur Radiol* 16:1898–1905

17. Marugami N, Tanaka T, Kitano S, Hirohashi S, Nishiofuku H, Takahashi A, Sakaguchi H, Matsuoka M, Otsuji T, Takahama J, Higashiura W, Kichikawa K (2009) Early detection of therapeutic response to hepatic arterial infusion chemotherapy of liver metastases from colorectal cancer using diffusion-weighted MR imaging. *Cardiovasc Intervent Radiol* 32:638–646
18. Rhee TK, Naik NK, Deng J, Atassi B, Mulcahy MF, Kulik LM, Ryu RK, Miller FH, Larson AC, Salem R, Omary RA (2008) Tumor response after yttrium-90 radioembolization for hepatocellular carcinoma: comparison of diffusion-weighted functional MR imaging with anatomic MR imaging. *J Vasc Interv Radiol* 19:1180–1186
19. Theilmann RJ, Borders R, Trouard TP, Xia G, Outwater E, Ranger-Moore J, Gillies RJ, Stopeck A (2004) Changes in water mobility measured by diffusion MRI predict response of metastatic breast cancer to chemotherapy. *Neoplasia* 6:831–837
20. Yuan Z, Ye XD, Dong S, Xu LC, Xu XY, Liu SY, Xiao XS (2009) Role of magnetic resonance diffusion-weighted imaging in evaluating response after chemoembolization of hepatocellular carcinoma. *Eur J Radiol*. doi:10.1016/j.ejrad.2009.05.040
21. Koh DM, Scurr E, Collins D, Kanber B, Norman A, Leach MO, Husband JE (2007) Predicting response of colorectal hepatic metastasis: value of pretreatment apparent diffusion coefficients. *AJR Am J Roentgenol* 188:1001–1008
22. Salem R, Thurston KG, Carr BI, Goin JE, Geschwind JF (2002) Yttrium-90 microspheres: radiation therapy for unresectable liver cancer. *J Vasc Interv Radiol* 13:S223–S229
23. Moffat BA, Chenevert TL, Lawrence TS, Meyer CR, Johnson TD, Dong Q, Tsien C, Mukherji S, Quint DJ, Gebarski SS, Robertson PL, Junck LR, Rehemtulla A, Ross BD (2005) Functional diffusion map: a noninvasive MRI biomarker for early stratification of clinical brain tumor response. *Proc Natl Acad Sci USA* 102:5524–5529
24. Moffat BA, Hall DE, Stojanovska J, McConville PJ, Moody JB, Chenevert TL, Rehemtulla A, Ross BD (2004) Diffusion imaging for evaluation of tumor therapies in preclinical animal models. *Magma* 17:249–259
25. Cui Y, Zhang XP, Sun YS, Tang L, Shen L (2008) Apparent diffusion coefficient: potential imaging biomarker for prediction and early detection of response to chemotherapy in hepatic metastases. *Radiology* 248:894–900
26. Thoeny HC, De Keyzer F, Chen F, Ni Y, Landuyt W, Verbeken EK, Bosmans H, Marchal G, Hermans R (2005) Diffusion-weighted MR imaging in monitoring the effect of a vascular targeting agent on rhabdomyosarcoma in rats. *Radiology* 234:756–764
27. Thoeny HC, De Keyzer F, Vandecaveye V, Chen F, Sun X, Bosmans H, Hermans R, Verbeken EK, Boesch C, Marchal G, Landuyt W, Ni Y (2005) Effect of vascular targeting agent in rat tumor model: dynamic contrast-enhanced versus diffusion-weighted MR imaging. *Radiology* 237:492–499
28. Jordan BF, Runquist M, Raghunand N, Baker A, Williams R, Kirkpatrick L, Powis G, Gillies RJ (2005) Dynamic contrast-enhanced and diffusion MRI show rapid and dramatic changes in tumor microenvironment in response to inhibition of HIF-1alpha using PX-478. *Neoplasia* 7:475–485
29. van Rijswijk CS, Kunz P, Hogendoorn PC, Taminiau AH, Doornbos J, Bloem JL (2002) Diffusion-weighted MRI in the characterization of soft-tissue tumors. *J Magn Reson Imaging* 15:302–307
30. Latour LL, Svoboda K, Mitra PP, Sotak CH (1994) Time-dependent diffusion of water in a biological model system. *Proc Natl Acad Sci USA* 91:1229–1233
31. Padhani AR, Liu G, Koh DM, Chenevert TL, Thoeny HC, Takahara T, Dzik-Jurasz A, Ross BD, Van Cauteren M, Collins D, Hammoud DA, Rustin GJ, Taouli B, Choyke PL (2009) Diffusion-weighted magnetic resonance imaging as a cancer biomarker: consensus and recommendations. *Neoplasia* 11:102–125